

F

Prof. Dr. K. Tesch

Internal Report
DESY D3-92
November 1998



X1998-01747

The residual radioactivity of a water-copper beam dump for the TESLA Test Facility

A. Leuschner and K. Tesch

Project	DESY
Date	11. NOV. 1998
Author	
Loan period	7 days

DESY behält sich alle Rechte für den Fall der Schutzrechtserteilung und für die wirtschaftliche Verwertung der in diesem Bericht enthaltenen Informationen vor.

DESY reserves all rights for commercial use of information included in this report, especially in case of filing application for or grant of patents.

**"Die Verantwortung für den Inhalt dieses
Internen Berichtes liegt ausschließlich beim Verfasser"**

Internal Report
DESY D3-92
November 1998

The residual radioactivity of a water-copper beam dump for the TESLA Test Facility

A. Leuschner and K. Tesch

Abstract:

Residual radioactivities induced in a dump for an electron beam of 2 GeV energy and 130 kW beam power are calculated. 42 nuclear reactions of photons, neutrons, and protons in water, copper, and carbon are considered which produce 10 long-living nuclides. Not all reaction cross-sections are available, missing values are estimated by approximations and extrapolations. The collected information on cross-sections is also useful for estimation of activities at much higher beam energies. The track lengths of the producing particles are calculated by a Monte Carlo code. Values for dose rates near the dump from residual activities are also given.

1. Introduction

The Linear Collider TESLA is proposed which collides beams of electrons and positrons with beam energies of 250 GeV each. One of the technical problems of this project is the absorption of the beam after having passed the interaction region. Only materials like water or carbon can withstand a beam power of 8 MW. A water dump has the advantage of smallest residual activity, it also needs simpler rotating fields to enlarge the diameter of the extremely thin incoming beam, as compared with a carbon dump. A drawback is the strong hydrolysis of water.

In order to study problems associated with a water dump it is proposed to construct a smaller water absorber and to test it at the TESLA Test Facility. The TTF is an electron linac which - at a later stage - will have an beam energy of 2 GeV and a mean beam power of 130 kW. A water-copper dump was proposed by Maslov et al. [1] ; in front of it a carbon beam spoiler is foreseen to increase the beam diameter. In the present report the calculation of residual activities in these 3 materials are described which are produced by photons, neutrons, and protons.

For calculating induced radioactivities one needs essentially the product of the tracklength of the producing particle in a specified material region multiplied with the reaction cross-section, integrated over the particle energy. In section 2 we compile and / or estimate reaction cross-sections leading to a specific radioactive nuclide for photons up to 1 GeV and for neutrons and protons up to 10 GeV. These energy ranges are large more than enough for an 2 GeV electron accelerator. The whole material is prepared to calculate radioactivities at a later stage for much higher electron beam energies, e.g. for 250 GeV. In section 3 the dump is described and examples of track length distributions are given. Resulting activities in water, copper and carbon are presented in section 4, section 5 gives some information on dose rates near the absorber.

2. Cross-sections

At high energy electron accelerators radioactive nuclides are produced by photons and by neutrons and protons which are created by the electromagnetic cascade. The number of produced nuclides can be large, in copper the production of about 60 unstable nuclei is possible. Fortunately most of them are unimportant in our case. We calculate the activities of only those radioactive nuclides which fulfill the following criterions :

- They are γ emitters.
- Their halflife is larger than 5 h.
- Their production cross-section is larger than 0.03 mb for photons and larger than 3 mb for protons in the proton energy range below 100 MeV.

We add the production of ^3H as it is a gas with long halflife.

The calculation of activities is simple in principle, the main problem is the fact that not all necessary cross-sections for reactions leading to a specific nuclide are experimentally determined. This incomplete knowledge is the largest source of error. Theoretical determination of nuclear reactions are possible taking into account the development of the intranuclear cascade at high energies. Such calculations give good results, e.g., about spectra of neutrons and protons leaving the nucleus. But the reliability of calculations of reaction cross-sections leading to a specified nuclide is not well established due to the sparsity of experimental data. An example is the PICA code [19] the results of which are not in good agreement with experiments [2, 3]. Therefore we use only experimental data together with simple extensions and extrapolations.

2.1. Copper cross-sections

In copper the production of 10 nuclides by photons, neutrons and protons is considered : ^{64}Cu , ^{60}Co , ^{58}Co , ^{57}Co , ^{56}Co , ^{54}Mn , ^{65}Zn , ^{62}Zn , ^7Be , ^3H . The behaviour of their production cross-sections as a function of energy is different for simple reactions and for spallation reactions.

First we discuss reactions induced by protons and neutrons. Here we have 5 simple reactions: $^{65}\text{Cu}(\text{p}, \text{pn})^{64}\text{Cu}$, $^{65}\text{Cu}(\text{n}, 2\text{n})^{64}\text{Cu}$, $^{63}\text{Cu}(\text{n}, \alpha)^{60}\text{Co}$, $^{65}\text{Cu}(\text{p}, \text{n})^{65}\text{Zn}$, $^{63}\text{Cu}(\text{p}, 2\text{n})^{62}\text{Zn}$. All their cross-sections have a pronounced peak between 10 and 20 MeV and a decreasing tail to higher energies. For protons the total curves including the tails are known up to proton

energies well above 100 MeV [4]. The neutron cross-sections are measured up to 20 MeV [5]. Since proton-induced and neutron-induced reactions do not differ too much at high energies we assume the same production cross-section for protons and neutrons above 50 MeV, and for neutrons a smooth transition between 20 and 50 MeV. The cross-section for $^{63}\text{Cu} (n, \gamma) ^{64}\text{Cu}$ is 4.5 b for thermal neutrons.

The other proton- and neutron-induced reactions leading from ^{63}Cu and ^{65}Cu to one of the above-mentioned 10 nuclides are spallation reactions. Their thresholds vary between 25 and 50 MeV (for production of ^7Be about 100 MeV), and they have a weakly pronounced maximum above threshold. All proton cross-sections except that for production ^3H are measured up to 10 GeV [4]. The reaction $\text{Cu} (p, x) ^3\text{H}$ is measured only at 12 and 25 GeV together with the corresponding reaction in aluminium, the Cu / Al ratio being 2.5. We take the other measured aluminium data and multiply them with the same ratio to receive a crude estimate of tritium production in copper. Again we assume that for all spallation reactions the cross-sections for protons and neutrons are the same.

Only little information is available about photon-induced reactions leading to the same nuclides in the energy range up to 1 GeV. Most of them are spallation reactions. The general behaviour of their cross-sections is the following. They increase above threshold within an energy intervall of about 40 MeV and then remain constant up to 200 MeV. Examples are $^{51}\text{V} (\gamma, \alpha 3n) ^{44}\text{Sc}$ [6] and $^{232}\text{Th} (\gamma, pxn)$ [7]. This behaviour is expected since in this energy range the quasi-deuteron spallation dominates the reaction, and the reaction $^2\text{H} (\gamma, n) p$ has an approximately constant cross-section between 100 and 300 MeV. Above 200 MeV the cross-sections rise again due to pion production having a broad resonance up to 400 MeV. For our reactions in copper we use two sources of experimental information. Shibata et al. [8] measured the cross-sections per equivalent photon for production of the 4 Co isotopes and of ^{54}Mn in copper up to 1 GeV. Assuming a $1/k$ photon spectrum one receives approximate values for the cross-sections per photon in the regions 100 - 250 MeV, 250 - 500 MeV, and 500 - 1000 MeV, they are listed in tab. 1. A compilation of cross-sections measured at Frascati is published in [9]. For a mean cross-section averaged in the intervall 300 - 1000 MeV and for medium-heavy target nuclei the authors find the expression

$$\bar{\sigma} = \frac{a \bar{\sigma}_N}{K \Delta Z} \exp(-C(A_p - A_s)^2); \quad A_s = 2.27 Z_p^{-2.2} \quad (1)$$

$$\Delta Z = Z_t - Z_p; \quad a = 4.26; \quad \bar{\sigma}_N = 258 \mu\text{b}; \quad K = 1.32; \quad C = 0.25$$

$A_p, Z_p = A$ and Z of the produced nucleus

$Z_t = Z$ of target nucleus

Unfortunately the averaging over the range 300 - 1000 MeV covers the contribution of the first pion resonance. Its importance can be seen in more detailed measurements of $^{118}\text{Sn}(\gamma, \text{pxn})$ or $^{51}\text{V}(\gamma, \text{xpy})$ performed at Lund [10] and at DESY [11]. If for the latter reactions the $\bar{\sigma}$ values from eq. 1 are calculated one finds an improvement if for the interval 250 - 500 MeV $\bar{\sigma}$ is multiplied by 1.5 and for 500 - 1000 MeV by 0.5. The resulting values are also entered into tab. 1 for our reactions in copper. Apparently the agreement between both sets of data is poor. We use average values indicated in the 3 last columns of tab.1 and a linear transition between threshold and 100 MeV.

A compilation of cross-sections for the production of ^7Be from medium-heavy nuclei appeared in [12]. The apparent experimental threshold is about 200 MeV. We take a value of $70\mu\text{b}$ for the range 250 - 1000 MeV. Cross-sections for photoproduction of ^3H are very low. We found rough mean values of $12\mu\text{b}$ between 20 and 50 MeV for nickel [13] and $6\mu\text{b}$ between 16 and 90 MeV for zinc [14]. We use $12\mu\text{b}$ in the interval 20 - 50 MeV, $5\mu\text{b}$ in 50 - 250 MeV, and $10\mu\text{b}$ in 250 - 1000 MeV for copper as a crude estimate.

A special case is the simple reaction $^{65}\text{Cu}(\gamma, n)^{64}\text{Cu}$. It will give the highest contribution to the total activity in copper. Its cross-section is known in the giant-resonance region [15]. Above 25 MeV and up to 140 MeV it is small and around 0.5 mb as can be seen from similar reactions like $^{39}\text{K}(\gamma, n)$ or $^{40}\text{Ca}(\gamma, \text{np})$ [16]. Above the mesonic threshold an increase is expected. Mean (γ, n) cross-sections in the interval 300 - 1000 MeV were measured at Frascati, from a compilation (17) valid for $A < 100$ the following expression is received for $\bar{\sigma}$ [mb]

$$\bar{\sigma}(\gamma, n) = 0.104 A^{0.81} \quad (2)$$

We use $\sigma = 4.5$ mb in the region 250 - 500 MeV and 1.5 mb in 500 - 1000 MeV to account for the effect of the pionic resonance (see above); this is in approximate agreement with [8].

The reactions $^{65}\text{Cu} (\gamma, \pi^-) ^{65}\text{Zn}$ and $^{63}\text{Cu} (\gamma, \pi^- n) ^{62}\text{Zn}$ are included in our calculations. We take the same cross-sections as those measured for the corresponding reactions on ^{51}V [18].

2.2. Cross-sections for carbon and oxygen

In carbon and water only two long-living nuclides can be produced : ^7Be and ^3H . The associated photoproduction cross-sections are experimentally determined up to about 100MeV [20-22]. The $^{12}\text{C} (\gamma, x) ^7\text{Be}$ reaction is measured between 300 and 1000 MeV (23), no other information is found about the effect of the pion resonance. So we proceed as in the previous subsection, and in analogy to corresponding cross-sections of heavier nuclei we assume the values shown in fig. 1 (the histograms are prepared according to the photon groups used in the Monte Carlo calculations of section 3).

Hadronic cross-section : For $^{12}\text{C} (p, x) ^3\text{H}$ values are compiled in [4], a theoretical calculation is also available [24]. The experimental values disagree; we take the more recent data of [25] since they are supported by the theoretical curve. For $^{12}\text{C} (n, x) ^3\text{H}$ we also accept the theoretical curve of [24]. Reliable data for $^{12}\text{C} (p, x) ^7\text{Be}$ are compiled in [4]. We assume the same values for $^{12}\text{C} (n, x) ^7\text{Be}$ since the calculations in [24] show only slight differences between the two production modes. Data for $^{16}\text{O} (p, x) ^3\text{H}$ are taken from [25]. For the corresponding neutron-induced reaction we use a curve of similar shape but somewhat higher values as shown for the tritium production from ^{12}C . The cross-sections for $^{16}\text{O} (p, x) ^7\text{Be}$ are taken from [4], we assume the same data for $^{16}\text{O} (n, x) ^7\text{Be}$. The hadronic cross-sections used for our calculations are displayed in fig. 2.

3. Track lengths

The composition of the proposed water-copper dump [1] was simplified so that it is suitable for track length calculations by means of a Monte Carlo code. Fig. 3 shows the reduced cylindrical version. The FLUKA 97 code [26] was used to calculate track lengths of photons, neutrons, and protons in all indicated regions. The surrounding concrete cylinder acts only as a backscatterer for neutrons, its residual activity is neglected in the present report.

Two examples of track length distributions are presented. Fig. 4 shows the distributions of photons, neutrons, and protons in the water (regions 7-11, see fig. 3), and fig. 5 those in the copper region 13 (with will turn out to have the highest activity in copper).

4. Calculated activities

The dump of the TTF is dimensioned for a 2 GeV electron beam with $4 \cdot 10^{14}$ e/s (130 kW). With cross section $\sigma(E)$ (cm²) of a secondary particle for a specified nuclear reaction and its track length distribution $dL(E)/dE$ (cm) in a given region of the dump, the saturation radioactivity A_s (Bq) is calculated by

$$A_s = 4 \cdot 10^{14} n \int_0^{E_0} \sigma(E) \frac{dL(E)}{dE} dE \quad (3)$$

$$n = \text{number of nuclei per cm}^3$$

The received A_s values for all considered nuclides in the carbon spoiler, the water and for the sum of all copper regions, produced by photons, neutrons and protons, are given in Tab. 2. For a given time t_1 of continuous accelerator operation and a decay time t_2 , the actual activities are easily calculated by

$$A(t_1, t_2) = A_s (1 - \exp(-\lambda t_1)) \exp(-\lambda t_2) \quad (4)$$

λ being the decay constant of the nuclide. The nuclides produced by different reactions are put together and compiled in tab. 3 for $t_1 = \infty$, $t_2 = 0$ (i.e. the saturation activity) and one realistic case with $t_1 = 100$ d ; $t_2 = 1$ d . (Note that for all $t_2 = 0$ cases more shortlived nuclides are present which are not considered in this paper).

Some general conclusions are drawn for a quick overview :

- (a) The relative contributions of photons, neutrons, and protons to the total activities are given in tab. 4. The activity distribution in copper depends on the producing particles : most of the photon-produced activities is in the backing plate (region 17), whereas neutrons and protons produce the highest activity in region 13.

- (b) The activity in copper is dominated by ^{64}Cu . Fortunately it has a rather short half-life of 12.7 h, after a decay time $t_2 = 4$ d its activity is roughly as high as those of the 4 cobalt isotopes.
- (c) For t_1 from 100 d to 5 a and $t_2 = 4$ d the dominating nuclides in carbon and water are ^7Be and in copper ^{58}Co and ^{57}Co ; the total activities are about $7 \cdot 10^{10}$ Bq in carbon, $3 \cdot 10^{11}$ Bq in water, $7 \cdot 10^{11}$ Bq in copper. The activities in water need special attention regarding handling and storage, especially because of the gaseous and long-living ^3H . Its activity is roughly $1 \cdot 10^{11}$ Bq which is $2 \cdot 10^4$ times the Freigrenze (exemption value) according to the German regulation.
- (d) The activities in copper are highest in regions 17 and 13. The specific activities in the latter are given in tab. 5 for the 6 most important nuclides and for 3 sets of parameters t_1 and t_2 .

5. Dose rates near the dump

The dose rate produced by ^7Be in water and by the 6 most important nuclides in copper at a distance of 1 m from the axis of the dump (without the concrete shield) near section 13 is estimated. The dose constants of the nuclides are taken from [27]. The extension of the materials and the absorption of the γ doses in the thick copper walls are taken into account approximately. $t_1 = 100$ d and $t_2 = 1$ d.

With these parameters the activity in copper produces a dose rate of 6 mSv/h. After a decay time t_2 of 100 d the dose rate is still 1.5 mSv/h. The contribution of ^7Be in the water is negligible because of the thick copper wall. The dose rates do not include the contributions due to the activation of the shielding walls.

If the water is collected in a separate thin-walled storage tank the dose rate at 1 m distance is 0.4 mSv/h.

6. References

1. M. Maslov et al., IHEP Protvino (July 1998)
2. G. J. Miller et al., Nucl. Phys. A 551 (1993) 135
3. T. Sato et al., Proc. 1. Intern. Workshop on EGS4, KEK Proc. 97-16 (1997), Tsukuba
4. Landolt-Börnstein, Numerical data in science and technology, NS,
Group I Vol. 13a (1991) + Vol. 13d (1994), Springer Verlag
5. V. Mc Lane et al., Neutron cross sections, Vol. 2, Academic Press.
6. R. A. Meyer et al., Nucl. Phys. A 122 (1968) 606
7. G. J. Miller et al., Nucl. Phys. A 551 (1993) 135
8. S. Shibata et al., Phys. Rev. C 35 (1986) 254
9. V. di Napoli et al., Lett. N. Cim. 21 (1978) 83
10. B. Bülow, Z. Phys. A 275 (1975) 261
11. I. Blomquist et al., Z. Phys. A 278 (1976) 83
12. V. di Napoli et al., CBPF, Rio de Janeiro, Report A 0027 (1977)
13. P. Kneisel et al., Z. Phys. 199 (1967) 440
14. L. A. Currie et al., Nucl. Phys. A 157 (1970) 49
15. S. S. Dietrich et al., At. Data Nucl. Data Tab. 38 (1988) 199
16. K. Kayser et al., Z. Phys. 239 (1970) 447
17. V. di Napoli et al., CBPF, Rio de Janeiro, reports A 0033 (1976), A 0026 (1977)
18. K. Sakamoto et al., Nucl. Phys. A 501 (1989) 693
19. C. Y. Fu et al., Conf. SATIF 3, Sendai (1997)
20. H. Artus, Z. Phys. 189 (1966) 355
21. V. V. Balashov et al., Nucl. Phys. 27 (1961) 337
22. A. Goldmann et al., Z. Phys. 192 (1966) 282
23. V. di Napoli et al., N. Cim. 55 B (1968) 95
24. S. Pearlstein, Health Phys. 65 (1993) 185
25. S. T. Kruger et al., Phys. Rev. C7 (1973) 2179
26. A. Fasso, A. Ferrari, P. Sala, J. Rauff, FLUKA 97
27. R. Dorner et al., Physik Daten 28-3 (1986), Fachinformationszentrum Karlsruhe

Produced nuclide	Cross section (mb)							
	100 - 250 MeV	Ref. 8 250 - 500 MeV	500 - 1000 MeV	Ref. 9, modif. 250- 500 MeV	500 - 1000 MeV	100 - 250 MeV	Average 250 - 500 MeV	500 - 1000 MeV
⁶⁰ Co	0.22	0.66	0.06	0.77	0.26	0.2	0.7	0.15
⁵⁸ Co	0.38	1.1	0.48	0.70	0.23	0.4	0.9	0.35
⁵⁷ Co	0.43	0.76	0.26	0.31	0.10	0.4	0.5	0.15
⁵⁶ Co	0.13	0.30	0.14	0.085	0.03	0.1	0.2	0.1
⁵⁴ Co	0.23	0.75	0.39	0.50	0.16	0.2	0.6	0.3

Tab. 1 Photon-induced reaction cross sections for copper in 3 energy intervalls.

Material	Reaction	A _s (Bq)
Carbon	C (γ, x) ³ H	4.6 + 10
	C (γ, x) ⁷ Be	5.8 + 10
	C (n, x) ³ H	8.7 + 9
	C (n, x) ⁷ Be	4.8 + 9
	C (p, x) ³ H	2.5 + 9
	C (p, x) ⁷ Be	2.2 + 9
Water	O (γ, x) ³ H	5.0 + 11
	O (γ, x) ⁷ Be	1.4 + 11
	O (n, x) ³ H	1.5 + 11
	O (n, x) ⁷ Be	3.6 + 10
	O (p, x) ³ H	2.1 + 10
	O (p, x) ⁷ Be	9.2 + 9
Copper	⁶⁵ Cu (γ, n) ⁶⁴ Cu	6.8 + 12
	Cu (γ, x) ⁶⁰ Co	2.1 + 10
	Cu (γ, x) ⁵⁸ Co	3.2 + 10
	Cu (γ, x) ⁵⁷ Co	3.0 + 10
	Cu (γ, x) ⁵⁶ Co	6.2 + 9
	Cu (γ, x) ⁵⁴ Mn	1.3 + 10
	Cu (γ, x) ³ H	3.7 + 9
	Cu (γ, x) ⁷ Be	3.0 + 8
	⁶⁵ Cu (γ, π ⁻) ⁶⁵ Zn	5.0 + 8
	⁶³ Cu (γ, π ⁻ n) ⁶² Zn	8.8 + 8
	⁶⁵ Cu (n, 2n) ⁶⁴ Cu	9.2 + 11
	⁶³ Cu (n, α) ⁶⁰ Co	5.7 + 10
	Cu (n, x) ⁶⁰ Co	5.0 + 10
	Cu (n, x) ⁵⁸ Co	2.3 + 11
	Cu (n, x) ⁵⁷ Co	2.0 + 11
	Cu (n, x) ⁵⁶ Co	3.6 + 10
	Cu (n, x) ⁵⁴ Mn	3.7 + 10
	Cu (n, x) ³ H	1.3 + 11
	Cu (n, x) ⁷ Be	4.4 + 8
	⁶³ Cu (n, γ) ⁶⁴ Cu	9.3 + 12
	⁶⁵ Cu (p, pn) ⁶⁴ Cu	1.2 + 10
	Cu (p, x) ⁶⁰ Co	3.0 + 9
	Cu (p, x) ⁵⁸ Co	1.2 + 10
	Cu (p, x) ⁵⁷ Co	1.2 + 10
	Cu (p, x) ⁵⁶ Co	2.8 + 9
	Cu (p, x) ⁵⁴ Mn	3.7 + 9
	Cu (p, x) ³ H	8.4 + 9
Cu (p, x) ⁷ Be	1.3 + 8	
⁶⁵ Cu (p, n) ⁶⁵ Zn	1.3 + 9	
⁶³ Cu (p, 2n) ⁶² Zn	2.0 + 9	

Tab. 2 Calculated saturation activities A_s.

Material	Produced nuclide	Activity (Bq)	
		$t_1 = \infty$ $t_2 = 0$	100 d 1 d
Carbon	^3H	$5.7 + 10$	$8.7 + 8$
	^7Be	$6.5 + 10$	$4.7 + 10$
Water	^3H	$6.7 + 11$	$1.0 + 10$
	^7Be	$1.8 + 11$	$1.3 + 11$
Copper	^{64}Cu	$1.7 + 13$	$4.6 + 12$
	^{60}Co	$1.3 + 11$	$4.6 + 9$
	^{58}Co	$2.7 + 11$	$1.7 + 11$
	^{57}Co	$2.4 + 11$	$5.4 + 10$
	^{56}Co	$4.5 + 10$	$2.6 + 10$
	^{54}Mn	$5.4 + 10$	$1.1 + 10$
	^3H	$1.4 + 11$	$2.1 + 9$
	^7Be	$8.7 + 8$	$6.2 + 8$
	^{65}Zn	$1.8 + 9$	$4.4 + 8$
	^{62}Zn	$2.9 + 9$	$4.7 + 8$

Tab. 3. Calculated activities of 10 nuclides.

t_1 = time of continuous operation , t_2 = decay time.

Material	A (γ) : A (n) : A (p)
Carbon	1 : 0.1 : 0.05
Water	1 : 0.3 : 0.05
Copper, ^{64}Cu	1 : 0.1 : 0.002
Copper, all other nuclides	1 : 7 : 0.4

Tab. 4. Ratios of saturation activities produced by photons, by neutrons and by protons.

Nuclide	Specific activity (Bq/g)		
	$t_1 = \infty$ $t_2 = 0$	100 d 1 d	100 d 100 d
^{64}Cu	2.0 + 6	5.3 + 5	0
^{60}Co	1.3 + 5	4.6 + 3	4.3 + 3
^{58}Co	2.5 + 5	1.5 + 5	5.6 + 4
^{57}Co	2.2 + 5	5.0 + 4	4.0 + 4
^{56}Co	4.0 + 4	2.3 + 4	9.3 + 3
^{54}Mn	4.0 + 4	8.0 + 3	6.3 + 3

Tab. 5. Specific activities in copper region 13 for 3 sets of operation time t_1 and decay time t_2 .

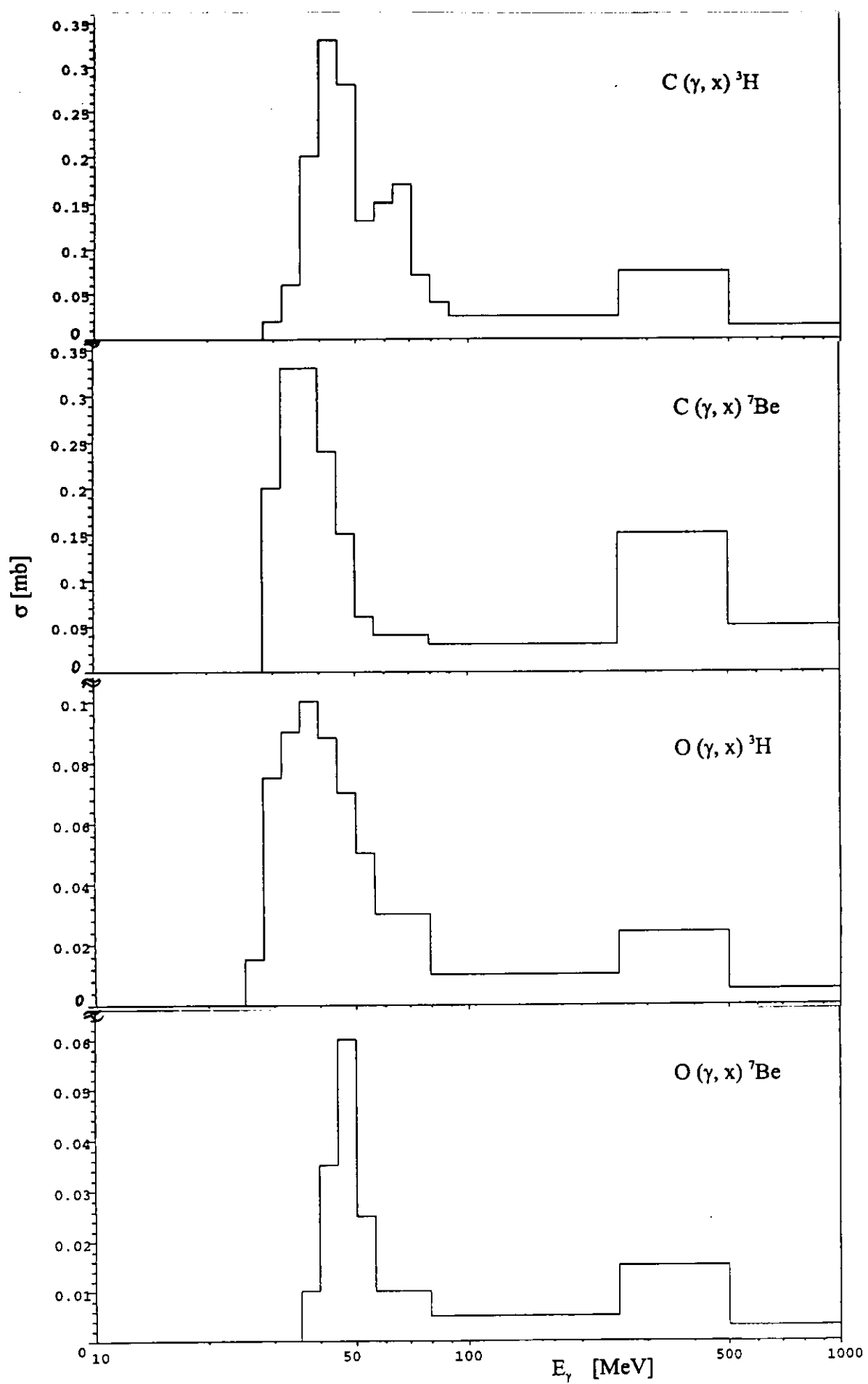


Fig. 1: Photoproduction cross-sections.

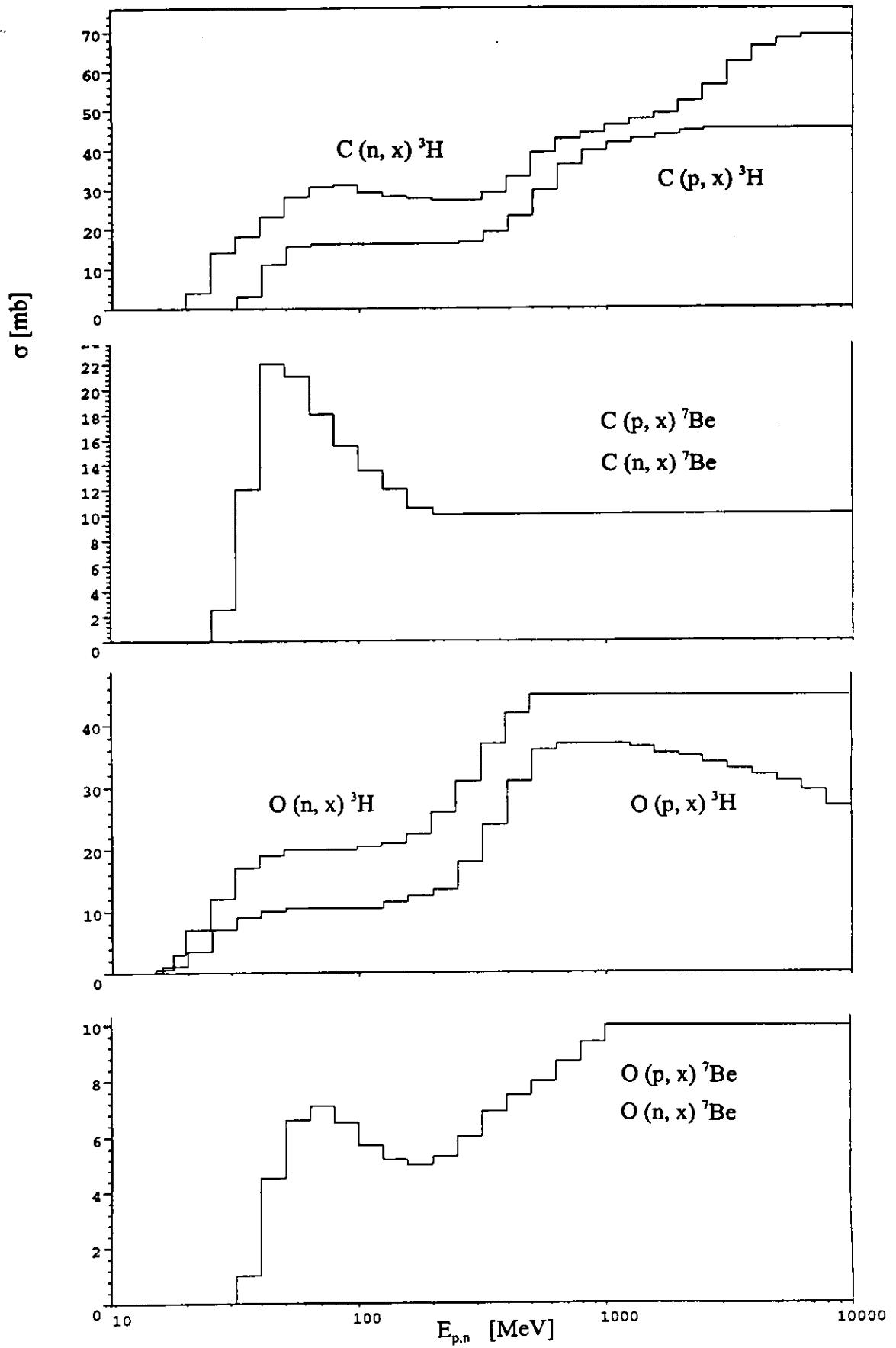


Fig. 2: Hadronic production cross-sections.

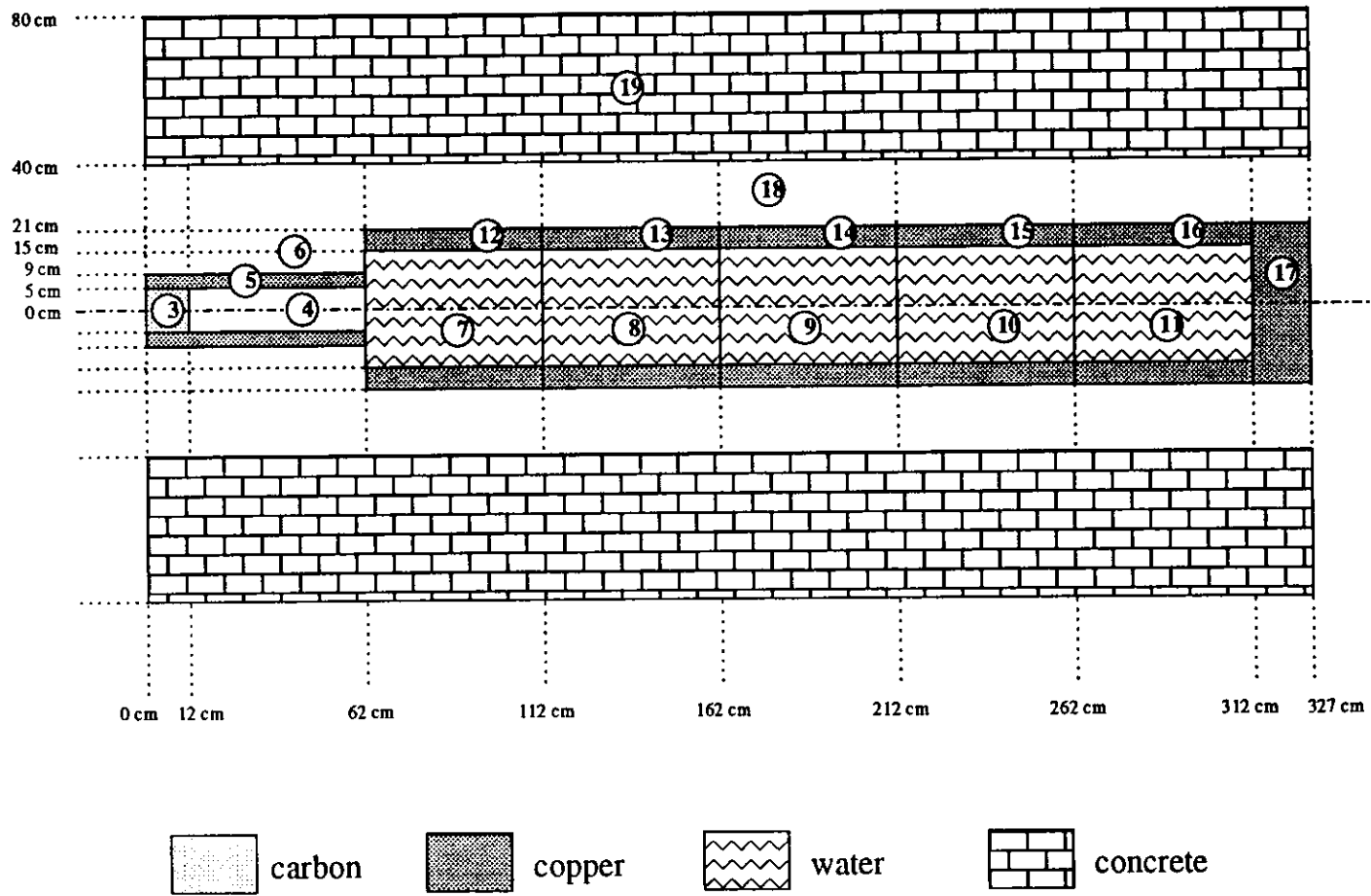


Fig.3: Simplified composition of the water-copper dump

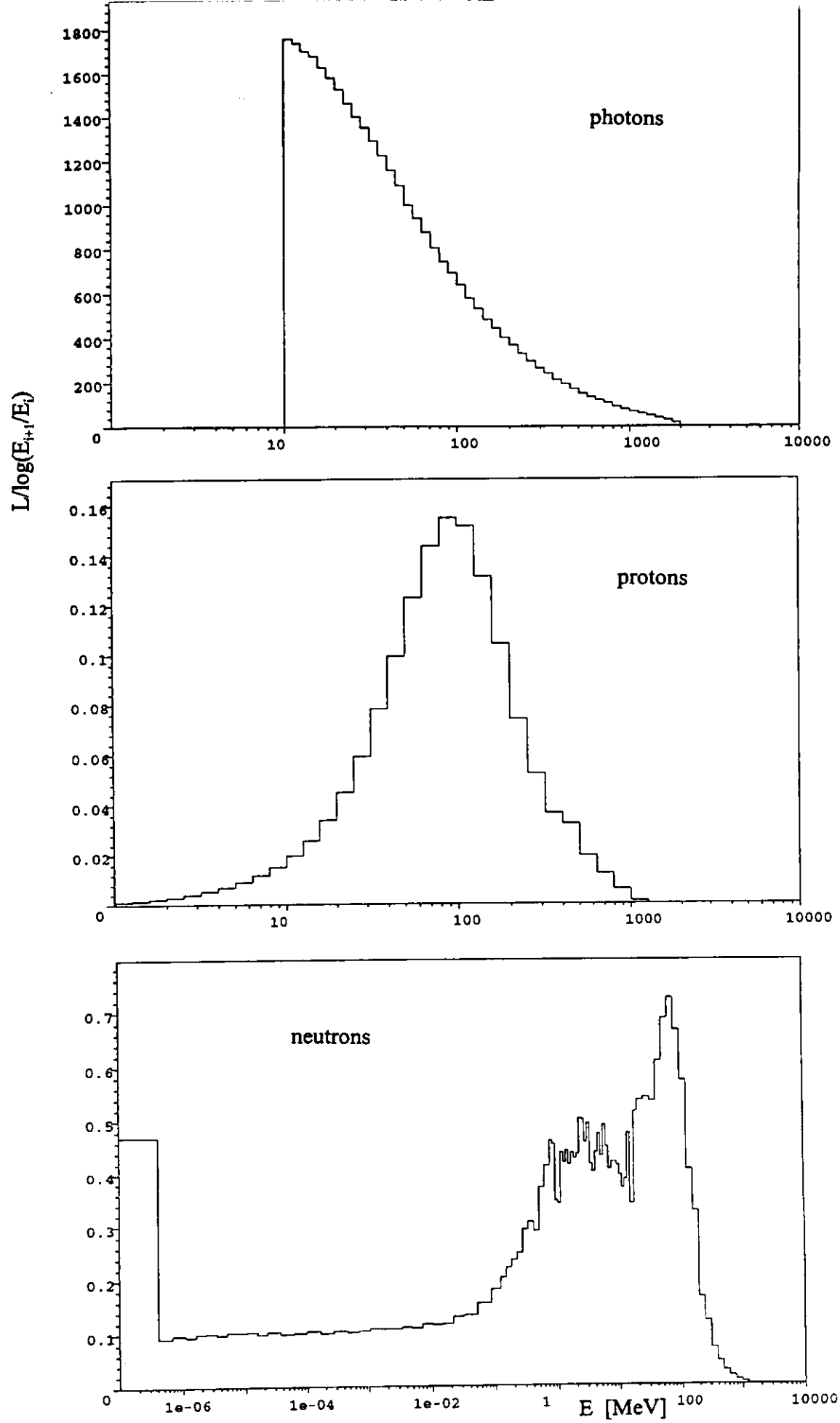


Fig. 4: Track lengths per logarithmic energy intervall in water.

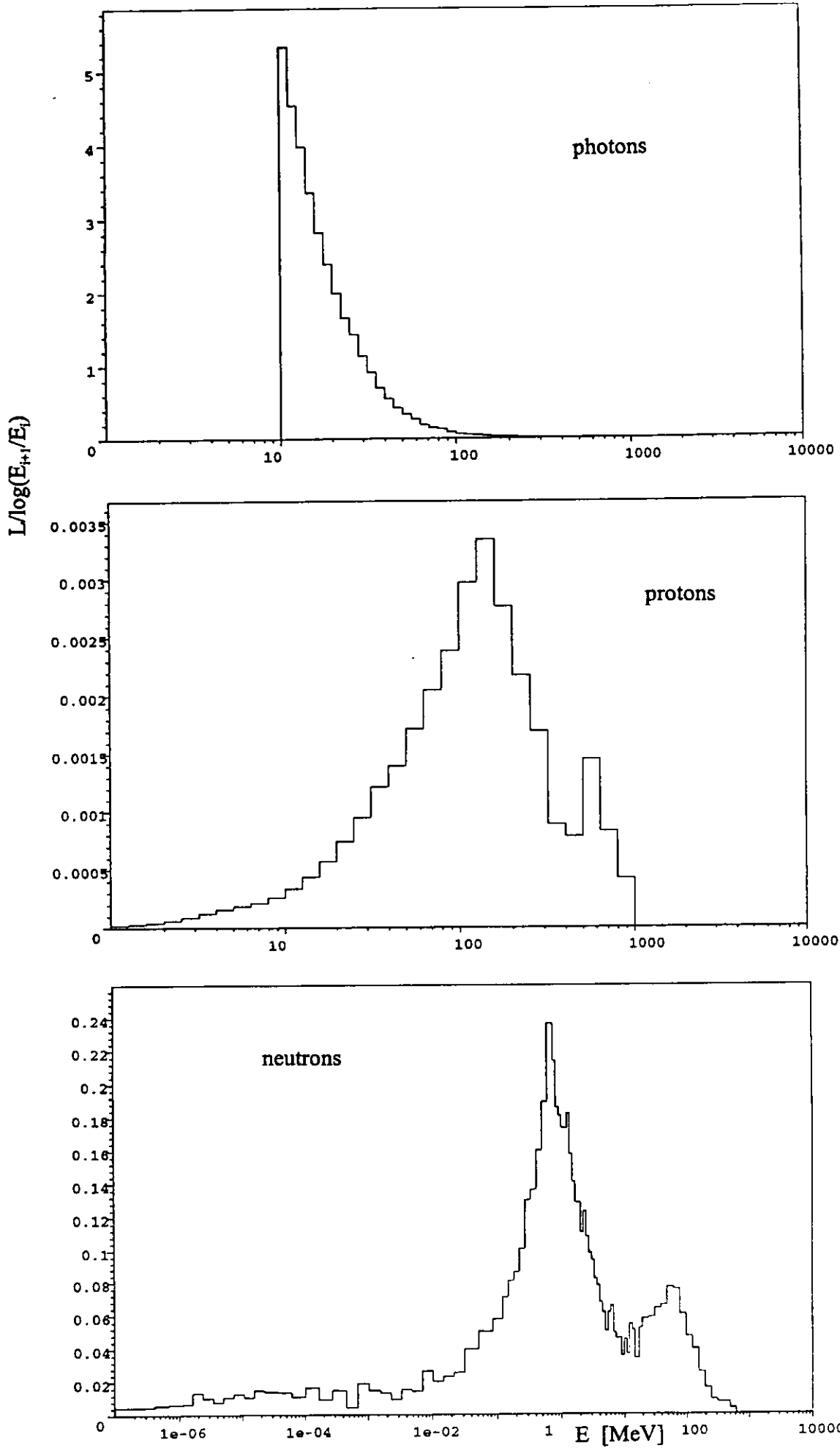


Fig. 5: Track lengths per logarithmic energy intervall in copper (region 13, see fig.3).